

# Influence of Osseointegration Degree and Pattern on Resonance Frequency in the Assessment of Dental Implant Stability Using Finite Element Analysis

Bin Deng, BDS, PhD<sup>1</sup>/Keson B. Tan, BDS (Hons), MSD<sup>2</sup>/Gui Rong Liu, PhD<sup>3</sup>/Yi Lu, BDS, PhD<sup>4</sup>

**Purpose:** Resonance frequency analysis (RFA) has been widely used to predict dental implant stability by assessing conditions surrounding the implant. The aim of this study was to investigate the influence of osseointegration degree and pattern on the resonance frequency of implant-bone structure by means of finite element analysis (FEA). **Materials and Methods:** A basic FEA model was created to represent a titanium implant in a portion of the maxillary bone at the left first premolar region. This model was then used to compute the vibration behaviors for 5 osseointegration degrees and 8 osseointegration pattern models using modal and harmonic analysis. **Results:** In the arbitrarily set osseointegration pattern models, a significant influence of osseointegration degree on the resonance frequency ( $P < .001$ ) could be expressed as the linear function  $R^2 = 0.99$ . No significant influence from the osseointegration pattern could be observed ( $P = .89$ ). While the coronal-osseointegration model had a slightly higher resonance frequency than others and the apical-osseointegration model had the lowest, the difference between the highest and lowest value was within 5% ( $P = .51$ ). In the randomly set osseointegration models, the osseointegration degree had a statistically significant influence on the resonance frequency ( $P < .001$ ); the pattern of random osseointegration for a certain osseointegration degree had little influence. **Conclusion:** It seems that RFA can detect implant-stability changes related to the increase in osseointegration degree. However, careful consideration should be given to its use in predicting the stability in vivo of loss of osseointegration at the marginal bone. *INT J ORAL MAXILLOFAC IMPLANTS* 2008;23:1082–1088

**Key words:** finite element analysis, implant stability, osseointegration, resonance frequency analysis

Resonance frequency analysis (RFA) has been proposed to identify the factors, including surgical technique,<sup>1–3</sup> loading protocol,<sup>4,5</sup> implant design,<sup>6–10</sup> and implant boundary condition,<sup>11–14</sup> that govern implant stability. From a biomechanical standpoint, the implant's boundary condition is a key factor of

resonance frequency. A dental implant inserted in soft jawbone should have a lower resonance frequency value, which suggests that the lower interface restriction would result in reduced primary implant stability.<sup>15–18</sup> In addition, studies have shown that loss of marginal bone can lead to a decrease in implant stability.<sup>14,19,20</sup>

Implant stability can also vary with a change in osseous remodeling and percentage of implant-bone interfacial tissue contact. The influence of mechanical property of this interfacial layer can be assessed by considering a change of stiffness during osseointegration.<sup>11,21–25</sup> The experimental outcomes on this topic indicated that an increase in stiffness of the interface would lead to increase in implant stability.<sup>11,20,26–28</sup> An uncertain degree and pattern of osseointegration can occur in various situations.<sup>29–33</sup> They are difficult to ascertain, owing to lack of noninvasive and precise assessment means. To date, few attempts have been made to determine their influ-

<sup>1</sup>Research Fellow, Department of Mechanical Engineering, National University of Singapore, Singapore.

<sup>2</sup>Associate Professor, Department of Restorative Dentistry, Faculty of Dentistry, National University of Singapore, Singapore.

<sup>3</sup>Professor, Department of Mechanical Engineering, National University of Singapore, Singapore; Professor, the Singapore-MIT Alliance (SMA), Singapore.

<sup>4</sup>Associate Professor, Department of Restorative Dentistry, Faculty of Stomatology, Xi'an Jiao Tong University, Xi'an, PR China.

**Correspondence to:** Dr Bin Deng, Center for Advanced Computations in Engineering Science (ACES), Department of Mechanical Engineering, National University of Singapore, 10 Kent Ridge Crescent, Singapore, 119260. Fax: +65-6516 4795. E-mail: dengbinny@yahoo.com

ences on the implant stability. An investigation of the healing patterns of functionally loaded implants still requires longitudinal histological and nondestructive biomechanical evaluations.<sup>34–36</sup>

Recently, 3-dimensional finite element analysis (3D FEA) has been used to effectively analyze the vibration behavior of dental implants. This is because of its ability to model complex structure and simulate field variables, which are difficult to replicate in *in vivo* or *in vitro* investigations.<sup>13,16,25,37</sup> By means of a 3D FEA approach, with this study, the authors hoped to gain more insight into the vibration behaviors of dental implant-bone structure and correlate computed resonance frequency with osseointegration degree and pattern.

## MATERIALS AND METHODS

The proposed solving procedure includes 3 steps:

1. 3D FEA modeling of dental implant-bone structures with various osseointegration degrees and patterns is performed.
2. Modal analysis is conducted to determine the nature frequency and corresponding modal shape. It is a starting point for the harmonic response analysis.
3. Harmonic response analysis is used to determine the steady-state response of the implant-bone structure to sustained cyclic loads that vary sinusoidally with time. The resonance frequencies of the structure can then be obtained by identifying the frequency at which the peak response quantity of displacements is obtained.

A basic 3D FEA model was created to present a 100% osseointegrated titanium dental implant in the maxillary left first premolar region (Fig 1). A finite element program (ANSYS 6.1, ANSYS, Canonsburg, PA, USA) was used to generate this model. The implant was 15 mm in length and 4 mm in diameter. The exposed height above the bone level was 1 mm. The configuration of the maxillary cancellous and cortical bone was modeled using computerized tomography of a 68-year-old patient. As presently defined, the mechanism of osseointegration is a very high rate of living bone modeling and remodeling within about 1 mm of the implant surface.<sup>22,38,39</sup> Within this model, a 0.2-mm layer of implant-bone interfacial tissue was created to simulate the biologic change of the interfacial tissue during the osseointegration process. The implant was to be inserted in the center of the alveolar ridge. The interfaces between the cortical and cancellous bone, cancellous bone and interfacial tissue, and implant and interfacial tissue were assumed perfectly bonded. This

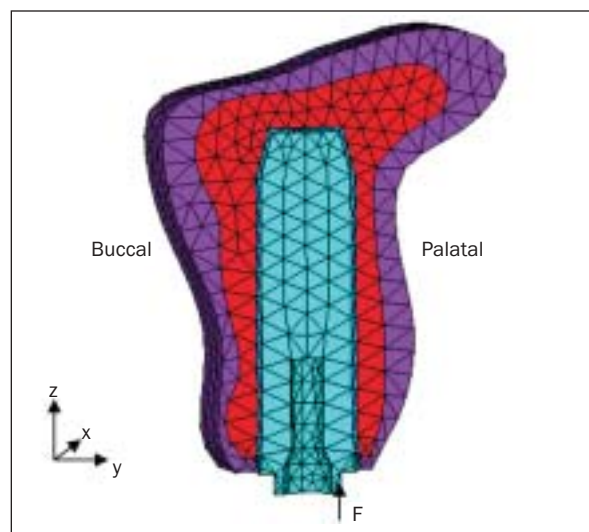


**Fig 1** Buccal-palatal section view of the basic 3D FEA model. An implant surrounded by a 0.2-mm layer of interfacial tissue is inserted in a portion of maxillary bone. F, force.

model was finely meshed with 10-node tetrahedral structurally solid elements. The mesh generation resulted in 6,259 elements and 9,909 nodes for every model with different osseointegration degrees and patterns.

The material properties of the cancellous and cortical bones are considered to be orthotropic and linearly elastic; they are presented in Table 1.<sup>40–42</sup> Young's modulus of 117,000 MPa, Poisson's ratio of 0.3, and density of 4.5 g/cm<sup>3</sup> were used for the titanium implant.<sup>16,43</sup>

Little is known about the mechanical property of the interfacial tissue at the level of detail needed for mechanical analysis.<sup>44</sup> From a mechanical point of view, however, different sets of elastic constants can be adopted to account for a wide range of conditions occurring in the implant-bone interfacial area.<sup>24,25</sup> In this study, 2 types of interfacial tissues differing in their elastic material properties were defined to describe the osseointegrated and nonosseointegrated interfacial tissues,<sup>33</sup> which are considered isotropic and linearly elastic. The histologic characteristics and mechanical properties of the interfacial tissues are presented in Table 2.

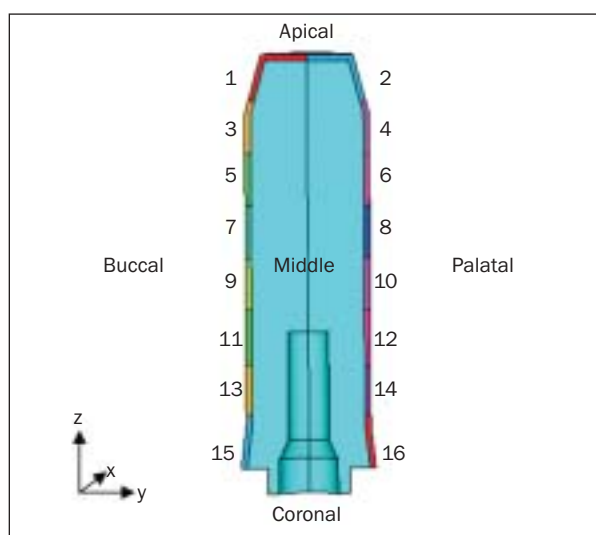
This basic model was then used to define different osseointegration degrees and patterns of the implant. Five osseointegration degrees—0%, 25%, 50%, 75%, and 100%—were assigned to the dental implants. To produce the 5 osseointegration degrees, the interfacial layer was divided arbitrarily into 32 segments. Each segment had the same volume. A buccal-palatal section is shown in Fig 2. The locations of the osseointegrated and nonosseointegrated areas were then assigned to the divided segments. Eight osseo-

**Table 1** Material properties of bone and implant used in the FEA model

Material	Young's modulus (MPa)			Shear modulus (MPa)			Poisson's ratio			Density (g/cm <sup>3</sup> ) $\rho$
	$E_x$	$E_y$	$E_z$	$G_{xy}$	$G_{yz}$	$G_{zx}$	$\nu_{xy}$	$\nu_{yz}$	$\nu_{zx}$	
Cancellous bone	346.8	457.2	1107.1	98.3	132.6	165.3	0.055	0.01	0.322	0.55
Cortical bone	11300	13800	19400	4100	4900	6200	0.274	0.273	0.237	1.94

**Table 2** Properties of implant-bone interfacial tissues

Tissue type	Histological description	Young's modulus (MPa)	Poisson's ratio	Density (g/cm <sup>3</sup> )
Nonosseointegrated	Provisional connective tissue	75	0.3	0.1
Osseointegrated	Formed bony tissue	480	0.3	0.5

**Fig 2** Buccal-palatal section view of the model with divided interfacial tissue around an implant. Mesial and distal direction is not depicted in the figure.

integration patterns were investigated in this study: apical osseointegration, buccal osseointegration, coronal osseointegration, middle osseointegration, palatal osseointegration, mesial osseointegration, distal osseointegration, and random osseointegration. Among them, the first 7 patterns were set arbitrarily. Random osseointegration was set randomly for 25%, 50%, and 75% osseointegration models.

For a certain osseointegration degree, the corresponding resonance frequency can be derived as the average of frequencies with the 7 osseointegration patterns (apical, buccal, coronal, middle, palatal, mesial, and distal). Similarly, for a particular osseointegration pattern, the corresponding frequency can be calculated by taking the mean of the 3 osseointegration degrees (25%, 50%, and 75%). It was noted that of the arbitrarily assigned 75% osseointegration models, only the apical, coronal, and middle parts of the interface were

osseointegrated. This means that 24 osseointegrated segments were assigned to each of the 3 parts. However, it is impractical to assign the same osseointegration degree to the buccal, palatal, mesial, and distal interfaces along the implant. Therefore, 4 models of these patterns were not created. The pattern of random osseointegration for the osseointegration degree of 25%, 50%, and 75% was further adopted to simulate the possible osseointegration that occurs in a clinical situation. If the osseointegration degree was assigned to 25%, 8 segments would be randomly selected from a distribution. Similarly, if the osseointegration degree was 50% or 75%, the number of selected segments would be 16 and 24, respectively. According to the central limit theorem,<sup>45</sup> 30 patterns generated using a random function were monitored. Correspondingly, 30 resonance frequencies at each osseointegration degree were collected and used for statistical analysis. The mean value of the 30 frequencies at each osseointegration degree were adopted to evaluate the influence of osseointegration degree on the resonance frequency.

Each FEA model was constrained in all 3 degrees of freedom at each of the nodes located at the external mesial-distal surfaces of the bone segment. Modal analysis was then used to determine the vibration characteristics, ie, natural frequencies and mode shapes, of the implant-bone structure. In the harmonic analysis, a vertical force of 10 N was applied to the end of the implant (node 779, Fig 1). The sweep frequency is based on the results obtained from the modal analysis. We focused on only the fundamental resonance frequency based on the fact that this frequency corresponds to that usually measured with experimental devices. The linear correlation between osseointegration degree and resonance frequency was analyzed. The influence of osseointegration degree and osseointegration pattern on the resonance frequency was analyzed by single-factor analysis of variance (ANOVA). A value of  $P < .05$  was statistically significant.

## RESULTS

### Modal Analysis of the Basic Model

All FEA models with different osseointegration degrees and patterns had the same first-order mode shape but different first nature frequency values. The first nature frequency of the basic model with 100% osseointegration was 34 kHz. Its corresponding mode shape is shown in Fig 3. The black dashed line represents the undeformed shape of the osseointegrated implant-bone structure. The colored shape gives the ultimate position of the implant, interfacial layer, and bones for the corresponding mode. Figure 3 also indicates that the deformation occurs mainly in the interfacial tissue and that the mode shape is a translation mode along the longitudinal axis of the implant in YZ plane.

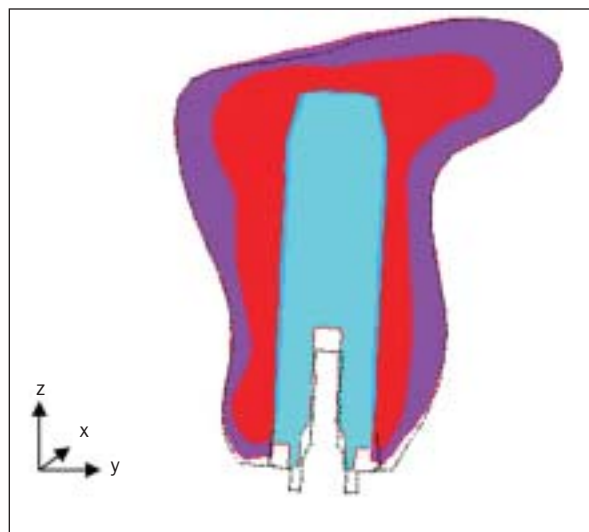
### Harmonics Response Analysis of the Basic Model

Figure 4 shows the forced harmonic response of the basic model. The fundamental resonance frequency of 33.9 kHz, very close to the first nature frequency, is found at its corresponding peak displacement. The resonance frequency of the other models can also be easily obtained with the same method.

### Influence of Osseointegration Degree and Pattern

Figure 5 shows that the osseointegration degree had a significant influence on the resonance frequency ( $P < .001$ ). When the osseointegration degree is 0%, the frequency is at the smallest value; when the osseointegration degree is 100%, the frequency reaches its highest value. The influence of osseointegration degree on the frequency follows the linear function  $R^2 = 0.99$ . Figure 6 indicates that the osseointegration pattern had no significant influence on the resonance frequency ( $P = .89$ ). However, the coronal osseointegration models had slightly higher resonance frequencies than others, and the apical osseointegration models had the lowest values. The difference between the highest and lowest value was within 5% ( $P = .51$ ).

For each osseointegration degree of 25%, 50%, and 75%, 30 samples were randomly chosen using a function. The result is illustrated in Fig 7 and summarized in Table 3. Obviously, the osseointegration degree had strong linear influence on the resonance frequency ( $P < .001$ ), while the random-osseointegration for the certain osseointegration degree had little influence. The results also indicate that there was no significant correlation between the osseointegration degree and osseointegration pattern on the resonance frequency.



**Fig 3** The first mode shape of the implant-bone system. This mode is a translation along the longitudinal axis of the implant in YZ plane.

## DISCUSSION

RFA has been used extensively to monitor implant stability under various clinical situations. With this method, implant stability is measured by determining the resonance frequency of the implant-bone system, which is mainly determined by the implant boundary conditions. Based on the definition of osseointegration,<sup>46</sup> it is commonly thought that a high level of direct implant-bone contact is advantageous for implant stability. Although experimental measurements provide limited information on conditions at the implant-tissue interface, the numerical simulation is useful to give relevant information about the interfacial interaction.<sup>25</sup> Using FEA, a geometrically refined model was developed in this study to evaluate the significance of different osseointegration degrees and osseointegration patterns that may exist but are difficult to approach clinically. Five osseointegration degrees from 0% to 100% were modeled by assigning various amounts of the formed mature bone at the implant's interface. Accordingly, this increased the implant-bone contact degrees. The results from the present study indicated an obvious trend of resonance frequency increase with increase of osseointegration degree, which is in agreement with the findings of previous studies.<sup>11,47-49</sup> By means of removal torque assessment and histological analysis, it has been demonstrated that an increase in implant stability with healing time could correlate with an increased degree of bone-implant contact. From a bioengineering perspective, the increase of the resonance frequency can be further explained by the vibration theory,<sup>50</sup> relating to increase of the stiffness of the implant-bone complex.

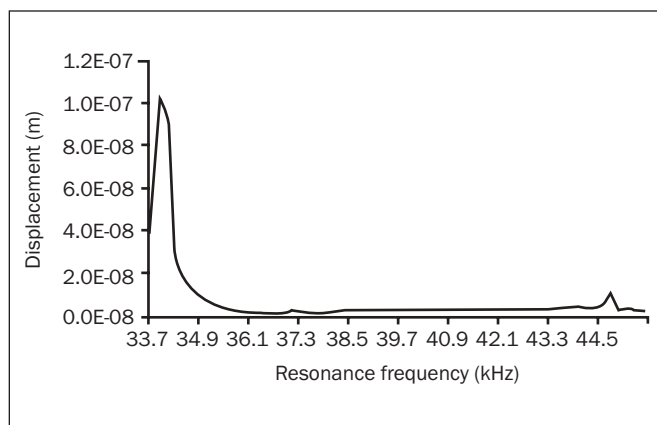


**Fig 4** Frequency spectrum of the basic model under the harmonic excitation at end of the implant (node 779). The first few resonance frequencies can be obtained by identifying the frequencies at the peak displacement points.

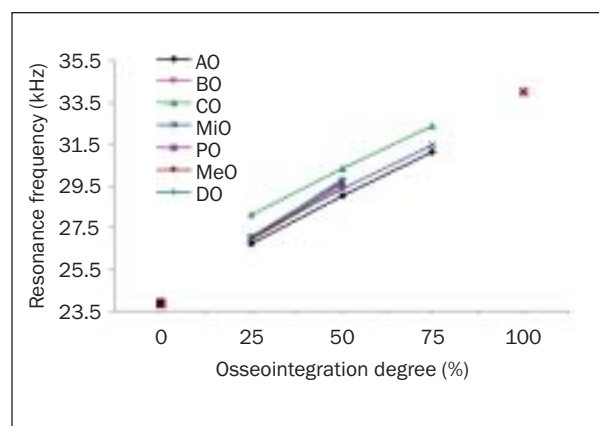


**Fig 5** Influence of osseointegration degree on the resonance frequency. AO, apical osseointegration; BO, buccal osseointegration; CO, coronal osseointegration; MiO, middle osseointegration; PO, palatal osseointegration; MeO, mesial osseointegration; DO, distal osseointegration.

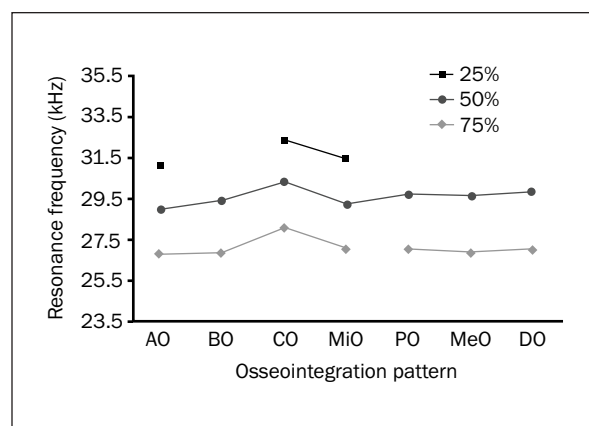


**Fig 6** Influence of the osseointegration pattern on the resonance frequency. AO, apical osseointegration; BO, buccal osseointegration; CO, coronal osseointegration; MiO, middle osseointegration; PO, palatal osseointegration; MeO, mesial osseointegration; DO, distal osseointegration.

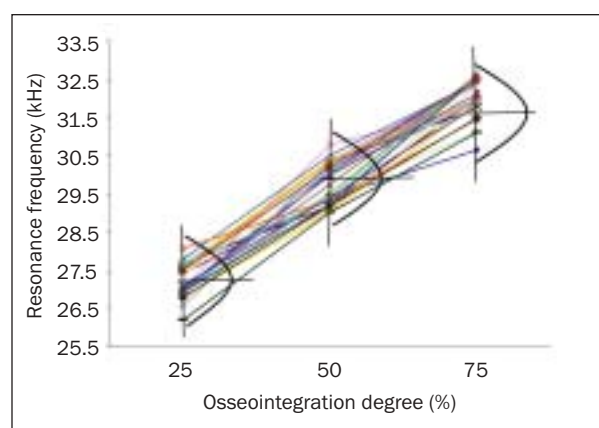


**Fig 7** Influence of 25%, 50%, and 75% osseointegration degrees on the resonance frequency.

**Table 3** The Resonance Frequency (kHz) of 3 Osseointegration Degrees Corresponding to the Randomly Selected Osseointegration Patterns

	Osseointegration degree		
	25%	50%	75%
Mean	27.2	29.8	32.0
SD	0.44	0.50	0.53
SD/mean	1.62%	1.68%	1.65%

SD, standard deviation.



During the healing process, the bony interface ratio may vary in portion and direction of osseointegrated implants for 3D morphometric observation.<sup>31,32</sup> In this study, 8 patterns of osseointegration were considered. No significant influence of the osseointegration pattern on the resonance frequency values could be observed. This is due to the overall stiffness and mass of the implant-bone system, which had no obvious change for any model of osseointegration pattern. It is clear from Figs 5 and 6 that the resonance frequency for the pattern of coronal osseointegration was slightly higher than that of other osseointegration patterns, which implies the importance of marginal bone support. The lowest resonance frequencies could be found in apical-osseointegration models, in which low levels of bony bonding existed around implants in the marginal portion. Further, these findings imply that loss of marginal bone is the most common cause of implant failure and is mainly related to overloading.<sup>51</sup> In the present study, a small decrease of 5% was found for the change from a coronal-osseointegration to an apical-osseointegration model. One should be careful to detect the loss of osseointegration in the marginal bone and predict implant stability in vivo based on the limited change of RFA measurements.

In the present study, the same implant type was used in the FEA computations. Of note, various implant designs (length, diameter, thread profile, and surface properties) are distinguished that lead to different host responses and implant stability. However, it is known from clinical measurement data that the ability of the RFA equipment to predict the influence of the implant designs is still a matter of debate. Sakoh et al<sup>52</sup> stated that no statistical differences with respect to primary stability could be found between a conical implant and a hybrid cylindric screw-type implant. Several reports have claimed no significant differences in the resonance frequency for the increase of the implant length and the diameter.<sup>7,11</sup> Nevertheless, Ostman et al<sup>10</sup> observed that there was a significant decrease of implant primary stability with increased implant length. Numerically, an evaluation of the influence of separate parameters of implant design indicated that an increase of implant length and diameter resulted in a decrease in the resonance frequency for an equal exposed implant height (Deng et al, unpublished data). Based on the basic theory of vibration, different implant designs should result in relative changes of the stiffness and mass of the whole implant-tissue system, thus affecting vibration. It can be expected that the possible correlation between implant design and stability will be elucidated by more fundamental numerical analyses and experimental observations.

## CONCLUSIONS

A 3D FEA model was constructed to investigate the influence of osseointegration degree and pattern on dental implant stability. Within the limitations of this study, the results show that increased osseointegration degree obviously increases the resonance frequency of the implant-bone system, yet the influence of osseointegration pattern is less notable. It can be concluded that the RFA technique is applicable to detect the implant stability changes related to the increase in osseointegration degree. However, the use of RFA measurements for predicting the stability in vivo should be given careful consideration in the situation of loss of osseointegration at the marginal bone.

## REFERENCES

1. Büchter A, Kleinheinz J, Wiesmann HP, et al. Biological and bio-mechanical evaluation of bone remodelling and implant stability after using an osteotome technique. *Clin Oral Implants Res* 2005;16:1–8.
2. Kim SK, Lee HN, Choi YC, Heo SJ, Lee CW, Choie MK. Effects of anodized oxidation or turned implants on bone healing after using conventional drilling or trabecular compaction technique: histomorphometric analysis and RFA. *Clin Oral Implants Res* 2006;17:644–650.
3. West JD, Oates TW. Identification of stability changes for immediately placed dental implants. *Int J Oral Maxillofac Implants* 2007;22:623–630.
4. Duyck J, R;139;nold HJ, Van Oosterwyck H, Naert I, Vander Sloten J, Ellingsen JE. The influence of static and dynamic loading on marginal bone reactions around osseointegrated implants: An animal experimental study. *Clin Oral Implants Res* 2001;12:207–218.
5. Nkenke E, Lehner B, Fenner M, et al. Immediate versus delayed loading of dental implants in the maxillae of minipigs: Follow-up of implant stability and implant failures. *Int J Oral Maxillofac Implants* 2005;20:39–47.
6. O'Sullivan D, Sennerby L, Meredith N. Measurements comparing the initial stability of five designs of dental implants: A human cadaver study. *Clin Implant Dent Relat Res* 2000;2:85–92.
7. Bischof M, Nedir R, Szmukler-Moncler S, Bernard JP, Samson J. Implant stability measurement of delayed and immediately loaded implants during healing. *Clin Oral Implants Res* 2004;15:529–539.
8. Akkocaoglu M, Uysal S, Tekdemir I, Akca K, Cehreli MC. Implant design and intraosseous stability of immediately placed implants: A human cadaver study. *Clin Oral Implants Res* 2005;16:202–209.
9. Al-Nawas B, Wagner W, Grötz KA. Insertion torque and resonance frequency analysis of dental implant systems in an animal model with loaded implants. *Int J Oral Maxillofac Implants* 2006;21:726–732.
10. Ostman PO, Hellman M, Wendelhag I, Sennerby L. Resonance frequency analysis measurements of implants at placement surgery. *Int J Prosthodont* 2006;19:77–83.
11. Meredith N, Alleyne D, Cawley P. Quantitative determination of the stability of the implant-tissue interface using resonance frequency analysis. *Clin Oral Implants Res* 1996;7:261–267.
12. Huang HM, Pan LC, Lee SY, Chiu CL, Fan KH, Ho KN. Assessing the implant/bone interface by using natural frequency analysis. *Oral Surg Oral Med Oral Pathol Oral Radiol Endod* 2000;90:285–291.

13. Pattijn V, Van Lierde C, Van der Perre G, Naert I, Vander Sloten J. The resonance frequencies and mode shapes of dental implants: Rigid body behaviour versus bending behaviour. A numerical approach. *J Biomech* 2006;39:939–947.
14. Lachmann S, Laval JY, Jäger B, et al. Resonance frequency analysis and damping capacity assessment. Part 2: Peri-implant bone loss follow-up. An in vitro study with the Periotest and Osstell instruments. *Clin Oral Implants Res* 2006;17:80–84.
15. Sennerby L, Meredith N. Resonance frequency analysis: measuring implant stability and osseointegration. *Compend Contin Educ Dent* 1998;19:493–502.
16. Huang HM, Lee SY, Yeh CY, Lin CT. Resonance frequency assessment of dental implant stability with various bone qualities: A numerical approach. *Clin Oral Implants Res* 2002;13:65–74.
17. Barewal RM, Oates TW, Meredith N, Cochran DL. Resonance frequency measurements of implant stability in vivo on implants with a sandblasted and acid-etched surface. *Int J Oral Maxillofac Implants* 2003;18:641–651.
18. Balshi SF, Allen FD, Wolfinger GJ, Balshi TJ. A resonance frequency analysis assessment of maxillary and mandibular immediately loaded implants. *Int J Oral Maxillofac Implants* 2005;20:584–594.
19. Rasmusson L, Stegersjö G, Kahnberg KE, Sennerby L. Implant stability measurements using resonance frequency analysis in the grafted maxilla: A cross-sectional pilot study. *Clin Implant Dent Relat Res* 1999;1:70–74.
20. Sennerby L, Persson LG, Berglundh T, Wennerberg A, Lindhe J. Implant stability during initiation and resolution of experimental periimplantitis: An experimental study in the dog. *Clin Implant Dent Relat Res* 2005;7:136–140.
21. Brunski JB. Biomechanical factors affecting the bone-dental implant interface. *Clin Mater* 1992;10:153–201.
22. Albrektsson T, Berglundh T, Lindhe J. Osseointegration: Historic background and current concepts. In: Lindhe J, Karring T, Lang NP (eds). *Clinical Periodontology and Implant Dentistry*. Oxford; Malden: Blackwell Science, 2003:809–820.
23. Huang HM, Chiu CL, Yeh CY, Lin CT, Lin LH, Lee SY. Early detection of implant healing process using resonance frequency analysis. *Clin Oral Implants Res* 2003;4:437–443.
24. Natali AN, Pavan PG, Ruggero AL. Analysis of bone-implant interaction phenomena by using a numerical approach. *Clin Oral Implants Res* 2006;17:67–74.
25. Natali AN, Pavan PG, Schileo E, Williams KR. A numerical approach to resonance frequency analysis for the investigation of oral implant osseointegration. *J Oral Rehabil* 2006;33:674–681.
26. Nkenke E, Hahn M, Weinzierl K, Radespiel-Tröger M, Neukam FW, Engelke K. Implant stability and histomorphometry: A correlation study in human cadavers using stepped cylinder implants. *Clin Oral Implants Res* 2003;14:601–609.
27. Sul YT, Johansson CB, Jeong Y, Wennerberg A, Albrektsson T. Resonance frequency and removal torque analysis of implants with turned and anodized surface oxides. *Clin Oral Implants Res* 2002;13:252–259.
28. Böchter A, Joos U, Wiesmann HP, Seper L, Meyer U. Biological and biomechanical evaluation of interface reaction at conical screw-type implants. *Head Face Med* 2006;2:5.
29. Roberts WE. Bone tissue interface. *J Dent Educ* 1988;52:804–809.
30. Barth E, Johansson C, Albrektsson T. Histologic comparison of ceramic and titanium implants in cats. *Int J Oral Maxillofac Implants* 1990;5:227–231.
31. Sahin S, Akagawa Y, Wadamoto M, Sato Y. The three-dimensional bone interface of an osseointegrated implant. II: A morphometric evaluation after three months of loading. *J Prosthet Dent* 1996;76:176–180.
32. Wadamoto M, Akagawa Y, Sato Y, Kubo T. The three-dimensional bone interface of an osseointegrated implant. I: A morphometric evaluation in initial healing. *J Prosthet Dent* 1996;76:170–175.
33. Papavasiliou G, Kamposiora P, Bayne SC, Felton DA. 3D-FEA of osseointegration percentages and patterns on implant bone interfacial stresses. *J Dent* 1997;25:485–491.
34. Meredith N, Shagaldi F, Alleyne D, Sennerby L, Cawley P. The application of resonance frequency measurements to study the stability of titanium implants during healing in the rabbit tibia. *Clin Oral Implants Res* 1997;8:234–243.
35. Scarano A, Degidi M, Iezzi G, Petrone G, Piattelli A. Correlation between implant stability quotient and bone-implant contact: A retrospective histological and histomorphometrical study of seven titanium implants retrieved from humans. *Clin Implant Dent Relat Res* 2006;8:218–222.
36. Schliephake H, Sewing A, Aref A. Resonance frequency measurements of implant stability in the dog mandible: experimental comparison with histomorphometric data. *Int J Oral Maxillofac Surg* 2006;35:941–946.
37. Williams KR, Williams AD. Impulse response of a dental implant in bone by numerical analysis. *Biomaterials* 1997;18:715–719.
38. Huja SS, Roberts WE. Mechanism of osseointegration: Characterization of supporting bone with indentation testing and backscattered imaging. *Seminars in Orthodontics* 2004;10:162–173.
39. Chang MC, Ko CC, Liu CC, Douglas WH, et al. Elasticity of alveolar bone near dental implant-bone interfaces after one month's healing. *J Biomech* 2003;36:1209–1214.
40. Dechow PC, Nail GA, Schwartz-Dabney CL, Ashman RB. Elastic properties of human supraorbital and mandibular bone. *Am J Phys Anthropol* 1993;90:291–306.
41. O'Mahony AM, Williams JL, Spencer P. Anisotropic elasticity of cortical and cancellous bone in the posterior mandible increases peri-implant stress and strain under oblique loading. *Clin Oral Impl Res* 2001;12:648–657.
42. Schwartz-Dabney CL, Dechow PC. Accuracy of elastic property measurement in mandibular cortical bone is improved by using cylindrical specimens. *J Biomech Eng* 2002;124:714–723.
43. Lang LA, Kang B, Wang RF, Lang BR. Finite element analysis to determine implant preload. *J Prosthet Dent* 2003;90:539–546.
44. Brunski JB, Puleo DA, Nanci A. Biomaterials and biomechanics of oral and maxillofacial implants: current status and future developments. *Int J Oral Maxillofac Implants* 2000;15:15–46.
45. Allan Gut. *Probability: A Graduate Course*. New York: Springer, 2005:329–382.
46. Brånemark PI. Introduction to osseointegration. In: Brånemark PI, Zarb GA, Albrektsson T (eds). *Tissue-integrated prostheses: Osseointegration in Clinical Dentistry*. Chicago: Quintessence, 1985:11–76.
47. Johansson CB, Albrektsson T. A removal torque and histomorphometric study of commercially pure niobium and titanium implants in rabbit bone. *Clin Oral Implants Res* 1991;2:24–29.
48. Sennerby L, Thomsen P, Ericson LE. A morphometric and biomechanical comparison of titanium implants inserted in rabbit cortical and cancellous bone. *Int J Oral Maxillofac Implants* 1992;7:62–71.
49. Brånemark R, Ohnrell LO, Nilsson P, Thomsen P. Biomechanical characterization of osseointegration during healing: An experimental in vivo study in the rat. *Biomaterials* 1997;18:969–978.
50. Fertis DG. *Mechanical and Structural Vibrations*. New York: Wiley, 1995:1–196.
51. Cehreli MC, Sahin S, Akça K. Role of mechanical environment and implant design on bone tissue differentiation: Current knowledge and future contexts. *J Dent* 2004;32:123–132.
52. Sakoh J, Wahlmann U, Stender E, Nat R, Al-Nawas B, Wagner W. Primary stability of a conical implant and a hybrid, cylindrical screw-type implant in vitro. *Int J Oral Maxillofac Implants* 2006;21:560–566.